



Numerical Analysis

Entropy-based nonlinear viscosity for Fourier approximations of conservation laws

Jean-Luc Guermond^{a,1}, Richard Pasquetti^b

^a *Department of Mathematics, Texas A&M University, College Station, TX 77843-3368, USA*

^b *Laboratoire J.A. Dieudonné, UMR CNRS 6621, Université de Nice-Sophia Antipolis, parc Valrose, 06108 Nice cedex 02, France*

Received 21 January 2008; accepted after revision 22 May 2008

Available online 20 June 2008

Presented by Olivier Pironneau

Abstract

An Entropy-based nonlinear viscosity for approximating conservation laws using Fourier expansions is proposed. The viscosity is proportional to the entropy residual of the equation (or system) and thus preserves the spectral accuracy of the method. **To cite this article:** *J.-L. Guermond, R. Pasquetti, C. R. Acad. Sci. Paris, Ser. I 346 (2008).*

© 2008 Académie des sciences. Published by Elsevier Masson SAS. All rights reserved.

Résumé

Une technique de viscosité entropique pour l'approximation de Fourier des lois de conservation. On propose une technique de viscosité non-linéaire entropique pour approcher les lois de conservation par une méthode spectrale Fourier. La viscosité est proportionnelle au résidu de l'équation d'évolution de l'entropie et est ainsi spectralement petite quand la solution est régulière. **Pour citer cet article :** *J.-L. Guermond, R. Pasquetti, C. R. Acad. Sci. Paris, Ser. I 346 (2008).*

© 2008 Académie des sciences. Published by Elsevier Masson SAS. All rights reserved.

Version française abrégée

On présente dans cette Note une technique pour résoudre les lois de conservation de la forme (1) par une méthode spectrale Fourier, cf. (3). La solution pouvant développer des chocs on introduit un terme de viscosité non-linéaire proportionnel au résidu de l'équation de conservation de l'entropie (4), (5). Les performances de la méthode sont d'abord validées pour l'équation de Burgers et pour un problème à flux non convexe (6). Les résultats obtenus sont présentés dans la Fig. 1. On considère ensuite le système des équations d'Euler (7), que l'on complète par des termes de viscosité similaires à ceux du système de Navier–Stokes, cf. (8), (9). Comme dans le cas scalaire, les viscosité et diffusivité artificielles sont proportionnelles au résidu de l'équation d'évolution de l'entropie, cf. (10) à (14). La technique est illustrée sur les tubes à choc de Lax, de Shu–Osher et de Woodward–Colella. Les résultats sont montrés dans la Fig. 2.

E-mail addresses: guermond@math.tamu.edu (J.-L. Guermond), Richard.Pasquetti@unice.fr (R. Pasquetti).

¹ Permanent address: LIMSI (CNRS-UPR 3251), BP 133, 91403 Orsay cedex, France.

Contrairement à d'autres approches plus standards, nous n'utilisons pas les variables entropiques, cf., par exemple, [1] ou [5]. Les viscosité et diffusivité artificielles sont directement construites sur l'équation d'évolution de l'entropie.

1. Introduction

Spectral methods are known to be ill-suited for approximating nonsmooth problems, the traditional example illustrating this point being the so-called Gibbs–Wilbraham phenomenon which arises when computing the Fourier expansion of a step function. It is generally believed that Spectral methods cannot approximate efficiently problems with shocks and sharp fronts. The goal of the present Note is to somewhat contradict this point of view and to introduce a stabilization technique for approximating nonlinear conservation laws using spectral methods. The key ingredient is a nonlinear viscosity which is proportional to the residual of the entropy equation.

The Note is organized as follows. We briefly review the literature in §2. The entropy-based nonlinear viscosity is described in §3. The performance of the method is illustrated by solving standard scalar conservation laws in §4. The extension of the method to the Euler system is detailed and illustrated in §5.

2. Literature background

One advantage of high-order methods over standard low-order methods is that they solve linear transport very accurately. For instance, the Fourier method solves exactly the linear transport problem in periodic domains whenever the initial data is in the span of the available Fourier modes and time is kept continuous. If the initial data cannot be represented exactly by the available Fourier modes but is nonetheless smooth, the approximation error is small and goes to zero faster than any power of N , N being the degree of the trigonometric approximation. The method is said to be spectrally accurate. High-order accuracy for the time approximation can be achieved by using a high-order time marching scheme, e.g. third or fourth order Runge–Kutta time integration (RK3, RK4). What essentially remains to be done for nonlinear conservation laws is to cure the Gibbs–Wilbraham phenomenon generated by shocks and other discontinuities and ascertain convergence to the entropy solution.

The Spectral Vanishing Viscosity (SVV) method, developed in the late 1980's [10] for periodic boundary conditions, is to the best of our knowledge one of the rare existing spectral technique that can solve hyperbolic PDEs without compromising spectral accuracy, i.e. the method converges exponentially fast if the solution is smooth. The main idea of SVV consists of augmenting the Fourier/Galerkin formulation by a viscous term that acts only on the high frequencies of the solution [10]. The method is known to be convergent for multi-dimensional scalar-valued nonlinear conservation laws [2]. It can be extended to nonperiodic problems [7] and is now used by some in the Large-Eddy Simulations [6,8] of turbulent flows.

The technique proposed in this Note is based on a nonlinear viscosity in the spirit of [1,5]. But contrary to [1,5], where the residual of the equation is used to construct the viscosity, we use the entropy equation (which is unambiguously defined for scalar conservation laws equipped with convex flux). This idea extends naturally to the Euler equations and more generally to systems that can be supplemented with one entropy equation. Moreover, when thinking of LES, this idea can be viewed as introducing an entropy sink in the Navier–Stokes equations in the spirit of [4], giving then a clear physical sense to this term.

The main difference between the present technique and the SVV approach is that the SVV viscosity is linear whereas the entropy-based viscosity is not. This difference translates into superior robustness. Moreover, just like the SVV approach, the present method can easily be extended to other kinds of spectral approximations.

3. Entropy-based vanishing viscosity for conservation laws

For the sake of simplicity, we restrict ourselves for the time being to one-dimensional scalar nonlinear conservation laws. The idea is extended to the Euler system in §5. With x and t being the independent space and time variables, we want to approximate the entropy solution to the following equation:

$$\partial_t u + \partial_x f(u) = 0, \quad u(x, 0) = u_0(x), \quad (x, t) \in [0, L] \times (0, +\infty), \quad (1)$$

equipped with periodic boundary conditions. The flux f is a smooth function. We assume that only one entropy pair $(E(u), F(u))$ is sufficient for selecting a unique entropy solution satisfying

$$\partial_t E(u) + \partial_x F(u) \leq 0, \quad (x, t) \in [0, L] \times (0, +\infty). \tag{2}$$

A Fourier approximation, $u_N = \sum_{|k| \leq N} \hat{u}_k(t) \exp(2i\pi kx/L)$, $\hat{u}_{-k} = \bar{\hat{u}}_k$, $i^2 = -1$, is defined by solving

$$\partial_t u_N + \partial_x P_N f(u_N) = \partial_x P_N (v_N(u_N) \partial_x u_N), \quad u_N(x, 0) = P_N u_0, \tag{3}$$

where P_N is the L^2 -projection onto trigonometric polynomial of degree N . (For the computations reported in this Note, the L^2 -projection of nonlinear terms is evaluated by using a pseudo-spectral method and the $\frac{3}{2}$ padding rule for de-aliasing.) The viscosity $v_N(u_N)$ is the critical ingredient of the algorithm. To construct $v_N(u_N)$, we first evaluate the residual of the entropy equation, which is obtained by augmenting (1) on the left-hand side with $-\partial_x(v(u)\partial_x u)$, multiplying the result by $E'(u)$, and recalling that $f'E' = F'$:

$$R(u_N) = \partial_t E(u_N) + \partial_x (F(u_N) - v_N(u_N) \partial_x E(u_N)) + v_N(u_N) E''(u_N) (\partial_x u_N)^2. \tag{4}$$

Then $v_N(u_N)$ is computed as follows:

$$v_N(u_N) = \min \left(v_{\max}, \alpha h \frac{|R(u_N)|}{\mathcal{N}(u_N)} \right), \tag{5}$$

where the mesh size h is defined by $h = L/2N$ and where α is a user-dependent constant; typically α can reasonably be chosen in the range $[0.02, 2]$ without that choice dramatically affecting the results. The quantity $\mathcal{N}(u_N)$ is a normalizing coefficient; in the examples below we used $E(u) = \frac{1}{2}u^2$ and set $\mathcal{N}(u_N) = \frac{1}{2}(\max |u_N|^2 - \min |u_N|^2)/L$. The purpose of v_{\max} is to limit the dissipation. Since $\max_{[u_{\min}, u_{\max}]} |f'(u_N)|$ is the maximum wave speed, we set $v_{\max} = \alpha_{\max} h \max_{[u_{\min}, u_{\max}]} |f'(u_N)|$, where α_{\max} is a user-dependent parameter (in practice $\alpha_{\max} \in [0.1, 2]$). v_{\max} is thus a limiting first-order artificial viscosity. Since the march in time is explicit, the time step δt must satisfy the stability restriction $v_{\max} \delta t \lesssim h^2$, which also can be rewritten $\delta t \lesssim h / \max_{[u_{\min}, u_{\max}]} |f'|$. As a result, the entropy viscous term introduces a standard CFL condition. In the tests reported below $v_N(u_N)$ is evaluated by using a pseudo-spectral method without de-aliasing.

Note that in the regions where the solution is smooth the entropy residual $R(u_N)$ is in principle small, whereas in shocks $R(u_N)$ is large. It is also clear that if the exact solution is smooth, $R(u_N)$ is spectrally small and the overall accuracy is spectral, i.e. the proposed method is formally spectrally accurate.

Finally, let us mention that since entropy should be produced only if $R(u_N)$ is positive, v_N could also be defined using the positive part of the entropy residual, $R(u_N)_+ := \frac{1}{2}(|R(u_N)| + R(u_N))$. We discuss this choice below.

4. Numerical tests for scalar conservation laws

We illustrate the capabilities of the above technique for solving various scalar conservation laws. The time integration is done using the strongly-stable explicit Runge–Kutta algorithm RK3 described in [3]. To compute the solution at the next time step, say t_{k+1} , the viscosity $v_N(u_N)$ is made explicit and evaluated at time t_k .

We first consider the Burgers equation, i.e. $f(u) = \frac{1}{2}u^2$, $E(u) = \frac{1}{2}u^2$, $F(u) = \frac{1}{3}u^3$, in the domain $[0, 1]$, i.e. $L = 1$, with the initial condition $u_0(x) = \sin(2\pi x)$. A stationary shock starts developing at time $t = 1/2\pi$ and is fully developed at $t = 0.25$. The solution u_N and the nonlinear viscosity $v_N(u_N)$, using $|R(u_N)|$, at $t = 0.25$ are reported in Fig. 1 for $N = 50, 100$, and 200 (these correspond to 100, 200, and 400 points, respectively). The graph of the solution is shown in the left panel and the viscosity $v_N(u_N)$ is shown in the center panel in log-scale. We used $\alpha_{\max} = 2$, $\alpha = 0.1$. The time step is recomputed at each time step so that $\text{CFL} = \max_{[u_{\min}, u_{\max}]} |f'(u_N)| \delta t / h = 0.1$. It is clear that the shock is well captured without oscillations and the nonlinear viscosity focuses on the shock. We have observed that the results are quite similar whether we use $|R(u_N)|$ or $R(u_N)_+$ in the definition of the nonlinear viscosity (5). The shocks are slightly sharper when using the positive part of the entropy residual, but overall $|R(u_N)|$ gives results that are more robust with respect to variations of the user-dependent parameter α .

To illustrate the robustness of the algorithm we consider a problem with nonconvex flux proposed in [9]:

$$f(u) = \begin{cases} \frac{1}{4}u(1-u) & \text{if } u < \frac{1}{2}, \\ \frac{1}{2}u(u-1) + \frac{3}{16} & \text{if } u \geq \frac{1}{2}, \end{cases} \quad \text{with initial data } u_0(x) = \begin{cases} 0, & x \in (0, 0.25], \\ 1, & x \in (0.25, 1]. \end{cases} \tag{6}$$

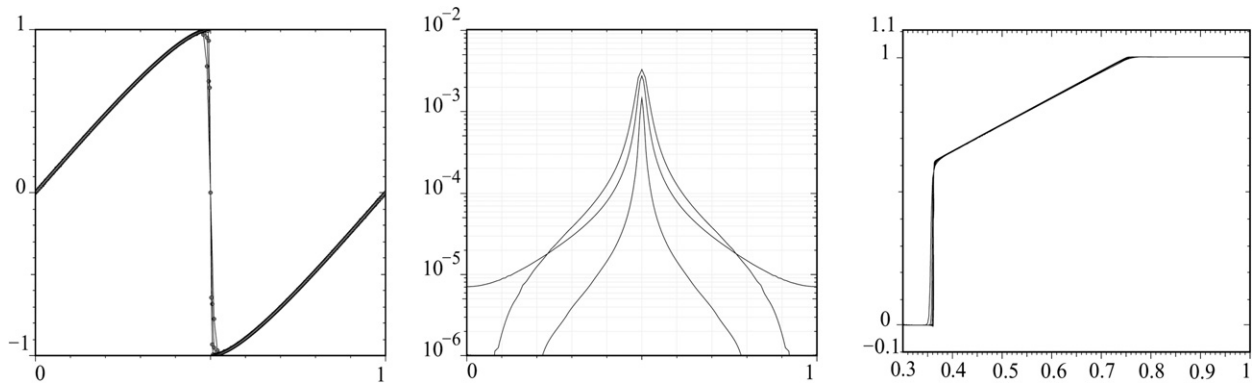


Fig. 1. Left: u_N and Center: $v_N(u_N)$, for Burgers at $t = 0.25$ with $N = 50, 100$, and 200 . Right: Nonconvex flux problem, u_N at $t = 1$ with $N = 200, 400, 800$, and 1600 .

Fig. 1. A gauche : u_N et au centre : $v_N(u_N)$, pour Burgers au temps $t = 0.25$. A droite : u_N pour le problème à flux non convexe à $t = 1$, pour différentes valeurs du paramètre de discrétisation N .

This problem is challenging since one entropy (say $u^2/2$) is not enough to uniquely define the entropy solution. Periodization is numerically forced by setting $u_0(0) = 1$. We show in Fig. 1 (right panel) the solution obtained at $t = 1$ for $N = 200, 400, 800$, and 1600 , using $|R(u_N)|$ in the definition for the nonlinear viscosity (5), the entropy pair $(E(u) = \frac{1}{2}u^2, F(u) = \frac{1}{3}u^3)$, and $\alpha_{\max} = 0.25, \alpha = 0.03$. The solution at time $t = 1$ is composed of a shock wave located at $\frac{1}{4}(\sqrt{6} - 1)$ followed by a rarefaction wave.

5. The Euler system

We now extend the method to the Euler equations of gas dynamics

$$\partial_t u(x, t) + \partial_x f(u(x, t)) = 0, \quad u = \begin{bmatrix} \rho \\ q \\ E \end{bmatrix}, \quad f(u) = \begin{bmatrix} q \\ qv + p \\ v(E + p) \end{bmatrix}, \tag{7}$$

where ρ is the density of the gas, v is the velocity, $q := \rho v$ is the momentum, E is the total energy per unit volume, and $p = (\gamma - 1)(E - \frac{1}{2}\rho v^2)$ is the pressure, $\gamma := 1.4$. The Euler system expresses the conservation of mass, momentum and energy for a perfect gas.

The natural question that arises at this point is the following: where should the nonlinear viscosity be introduced? To answer this question, we follow physics and look at the viscous case, that is at the Navier–Stokes system for which the momentum and energy equations are

$$\partial_t q + \partial_x(qv + p) = \partial_x(\mu \partial_x v), \tag{8}$$

$$\partial_t E + \partial_x((E + p)v) = \partial_x(\mu v \partial_x v) + \partial_x(\kappa \partial_x T), \tag{9}$$

where $T = p/\rho$ is the temperature, and μ and κ are the viscosity and conductivity, respectively. Note that all quantities are dimensionless and that a coherent choice of the reference values is assumed, so that the perfect gas constant equals 1. We then define a Fourier approximation to the Euler system by solving the Navier–Stokes system

$$\partial_t u_N + \partial_x P_N(f(u_N) + f_{\text{visc}}(u_N)) = 0, \quad f_{\text{visc}}(u_N) = \begin{bmatrix} 0 \\ -\mu_N(u_N) \partial_x v_N \\ -\mu_N(u_N) v_N \partial_x v_N - \kappa_N(u_N) \partial_x T_N \end{bmatrix}. \tag{10}$$

Following the same idea as for scalar conservation laws, we construct $\mu_N(u_N)$ and $\kappa_N(u_N)$ by using an entropy equation. It is known from thermodynamics that $S = \frac{\rho}{\gamma-1} \log(p/\rho^\gamma)$ is an entropy functional for perfect gases which satisfies the following balance equation

$$\partial_t S + \partial_x(vS - \kappa \partial_x \log(T)) = \mu \frac{(\partial_x v)^2}{T} + \kappa (\partial_x \log T)^2. \tag{11}$$

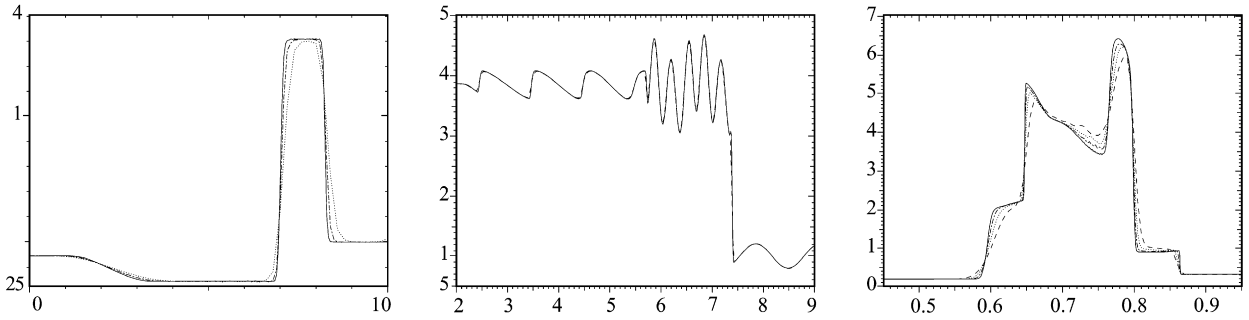


Fig. 2. Left: Lax shock tube, density at $t = 1.3$ for 50, 100 and 200 points. Center: Shu–Osher shock tube, density at $t = 1.8$, using 400 and 800 points. Right: Woodward–Collela shock wave, density at $t = 0.038$, using 200, 400, 800, and 1600 points.

Fig. 2. Masse volumique obtenue au temps t avec différentes discrétisations pour les tubes à choc de Lax (à gauche), de Shu–Osher (au centre) et de Woodward–Collela (à droite).

The discrete entropy residual is defined to be

$$R(u_N) = \partial_t S_N + \partial_x (v_N S_N - \kappa_N \partial_x \log(T_N)) - \mu_N \frac{(\partial_x v_N)^2}{T_N} - \kappa_N (\partial_x \log T_N)^2. \tag{12}$$

The quantity $|v_N| + (\gamma T_N)^{\frac{1}{2}}$ being the maximum wave speed, we construct a limiting viscosity as follows:

$$\mu_{\max} = \rho_N v_{\max}, \quad \text{where } v_{\max} = \alpha_{\max} h \max_x (|v_N(x)| + (\gamma T_N(x))^{\frac{1}{2}}). \tag{13}$$

Then $\mu_N(u_N)$ and $\kappa_N(u_N)$ are computed as follows:

$$\mu_N = \min(\mu_{\max}, \alpha h L |R(u_N)|), \quad \kappa_N = \beta \mu_N. \tag{14}$$

α_{\max} , α , and β are user-dependent parameters. In practice we have used, $\alpha_{\max} \in [\frac{1}{15}, \frac{1}{4}]$, $\alpha \in [\frac{1}{4}, 2]$ and $\beta \in (0, \frac{1}{4}]$. Note that we can also use the negative part of the entropy residual, $R(u_N)_-$, since definition (11) implies that S is an increasing quantity (we use the physical definition of the entropy). Our experience is that using $R(u_N)_-$ instead of $|R(u_N)|$ slightly sharpens shocks, although it is less robust (and using $R(u_N)_+$ produce oscillations, as expected). But, again, using $|R(u_N)|$ is slightly more robust since it can run with very small values of α . In the tests reported below $R(u_N)$ and $\mu_N(u_N)$ are evaluated by using a pseudo-spectral method without de-aliasing.

We now consider the following three standard test cases: the so-called Lax shock tube, the Shu–Osher shock tube and the Woodward–Collela shock wave problems. For the Lax shock tube the initial data are

$$\begin{cases} \rho = 0.445, & v = 0.698, & p = 3.528, & \text{if } x < 5, \\ \rho = 0.5, & v = 0, & p = 0.571, & \text{if } x > 5, \end{cases} \quad x \in [0, 10], \quad L = 10, \tag{15}$$

For the Shu–Osher shock tube the initial data are

$$\begin{cases} \rho = 3.857143, & v = 2.629367, & p = 10.333333, & \text{if } x < 1, \\ \rho = 1 + 0.2 \sin(5x), & v = 0, & p = 1, & \text{if } x > 1, \end{cases} \quad x \in [0, 10], \quad L = 10, \tag{16}$$

and for the Woodward–Collela shock wave the initial data are

$$\rho = 1, \quad v = 0, \quad \begin{cases} p = 1000, & \text{if } x < 0.1, \\ p = 0.01, & \text{if } 0.1 < x < 0.9, \\ p = 100, & \text{if } 0.9 < x < 1, \end{cases} \quad x \in [0, 1], \quad L = 1, \tag{17}$$

and the boundary conditions are $v|_{x=0} = 0$ and $v|_{x=1} = 0$ for all times. The Lax and Shu–Osher problems are made periodic by extending the domain to $[-10, 10]$ and making periodic extensions of the data. The Dirichlet boundary conditions for the Woodward–Collela problem are enforced by extending the domain to $[-2, 2]$ and appropriately extending the data.

The graph of the density at $t = 1.3$ for the Lax shock tube is shown in the left panel of Fig. 2 for three different resolutions, 50, 100 and 200 points (using $\alpha_{\max} = 0.2$, $\alpha = 1$, and $\beta = 0.1$). Both the shock and the contact discontinuity are well captured.

The graph of the density at $t = 1.8$ for the Shu–Osher shock tube is shown in the center panel of Fig. 2 for two different resolutions, 400 and 800 points respectively (using $\alpha_{\max} = 0.25$, $\alpha = 1$, and $\beta = 0.05$). This case is challenging since the fine features are very sensitive to any artificial viscosity.

The graph of the density at $t = 0.038$ for the Woodward–Collela shock wave is shown in the right panel of Fig. 2 for 200, 400, 800, and 1600 points (using $\alpha_{\max} = 0.15$, $\alpha = 0.15$, and $\beta = 0.05$). We observe convergence and the reader familiar with this problem will recognize that the limit solution is the correct one and the method performs quite well when compared with other standard (nonadaptive) techniques available in the literature.

Let us finally mention that sharper shocks and contact discontinuities can be obtained by using smaller coefficients α_{\max} , α and post-processing the solution very slightly. This will be explained elsewhere.

Acknowledgements

This material is based upon work supported by the National Science Foundation grants DMS-0510650 and DMS-0713829. The authors acknowledge insightful discussions with Bojan Popov.

References

- [1] R. Abgrall, Toward the ultimate conservative scheme: following the quest, *J. Comput. Phys.* 167 (2) (2001) 277–315.
- [2] G.-Q. Chen, Q. Du, E. Tadmor, Spectral viscosity approximations to multidimensional scalar conservation laws, *Math. Comp.* 61 (1993) 629–643.
- [3] S. Gottlieb, C.-W. Shu, E. Tadmor, Strong stability-preserving high-order time discretization methods, *SIAM Rev.* 43 (1) (2001) 89–112.
- [4] J.-L. Guermond, S. Prudhomme, On the construction of suitable solutions to the Navier–Stokes equations and questions regarding the definition of large eddy simulation, *Physica D* 207 (2005) 64–78.
- [5] C. Johnson, A. Szepessy, P. Hansbo, On the convergence of shock-capturing streamline diffusion finite element methods for hyperbolic conservation laws, *Math. Comp.* 54 (189) (1990) 107–129.
- [6] G.-S. Karamanos, G.E. Karniadakis, A spectral vanishing viscosity method for large-eddy simulations, *J. Comput. Phys.* 163 (2000) 22–50.
- [7] Y. Maday, M. Ould Kaber, E. Tadmor, Legendre pseudospectral viscosity method for nonlinear conservation laws, *SIAM J. Numer. Anal.* 30 (2) (1993) 321–342.
- [8] R. Pasquetti, Spectral vanishing viscosity method for large-eddy simulation of turbulent flows, *J. Sci. Comp.* 27 (1–3) (2006) 365–375.
- [9] G. Petrova, A. Kurganov, B. Popov, Adaptive semi-discrete central-upwind schemes for nonconvex hyperbolic conservation laws, *SIAM J. Sci. Comput.* 29 (6) (2007) 2381–2401.
- [10] E. Tadmor, Convergence of spectral methods for nonlinear conservation laws, *SIAM J. Numer. Anal.* 26 (1) (1989) 30–44.